DOI: 10.1021/ic902354e

Inorganic Chemistry
Article

Click-Triazole N2 Coordination to Transition-Metal Ions Is Assisted by a Pendant Pyridine Substituent

Damijana Urankar,[†] Balazs Pinter,[‡] Andrej Pevec,[†] Frank De Proft,*[,‡] Iztok Turel,[†] and Janez Košmrlj*[,†]

[†]*Faculty of Chemistry and Chemical Technology, University of Ljubljana, Aškerčeva 5, Ljubljana, Slovenia, and* [‡]*Faculteit Wetenschappen, Eenheid Algemene Chemie (ALGC), Vrije Universiteit Brussel (VUB), Pleinlaan 2, 1050 Brussels, Belgium*

Received November 27, 2009

We report that 1-(2-picolyl)-1,2,3-triazole (click triazole) forms stable complexes with transition-metal ions in which the coordination involves the triazole N2 nitrogen atom and the pendant 2-picolyl group. This is exemplified by model compound 1-(2-picolyl)-4-phenyl-1*H*-1,2,3-triazole ($\mathbf{L_x}$) and its complexes with transition-metal ions of Pt^{II}, Pd^{II}, Cu^{II}, Ru^{II}, and Ag^{I}. The coordination was investigated experimentally and theoretically. Ligand $\mathbf{L_x}$ easily reacted at room temperature with *cis*-$[PtCl_2(DMSO)_2]$, $[Pd(CH_3CN)_4](BF_4)_2$, $CuCl_2$, $[RuCl(\mu\text{-}Cl)(\eta^6\text{-}p\text{-cymene})]_2$, and $AgNO_3$ to give stable chelates $[PtCl_2\mathbf{L_x}]$ (**1**), $[Pd(\mathbf{L_x})_2](BF_4)_2$ (**2**), $[CuCl_2(\mathbf{L_x})_2]$ (**3**), $[RuCl(\eta^6\text{-}p\text{-cymene})\mathbf{L_x}]OTf$ (**4**), and $[Ag_2(\mathbf{L_x})_2(NO_3)_2]$ (**5**), respectively, in 60−98% yield. The structures of **1**−**5** were unambiguously confirmed by NMR spectroscopy and single-crystal X-ray diffraction analysis. Density functional theory calculations were carried out in order to theoretically investigate the stabilization factors in **1**−**5**. A comparison of the chelating properties of ligand $\mathbf{L_x}$ was made with structurally similar and isomeric 1-(2-aminoethyl)-substituted 1,2,3-triazole ($\mathbf{L_y}$) and 4-(2-aminoethyl)-substituted 1,2,3-triazole ($\mathbf{L_z}$). The complexation affinity of $\mathbf{L_x}$ was attributed to π-back-donation from the metal to the pendant pyridine side arm, whereas the stability of the complexes involving $\mathbf{L_y}$ and $\mathbf{L_z}$ mainly originates from efficient π-back-donation to the triazole ring.

Introduction

Commenced from its recent discovery, the copper-catalyzed azide−alkyne cycloaddition (CuAAC)[1] has emerged as a powerful and versatile tool in a wide variety of research areas, ranging from materials, to pharmaceuticals, to biological sciences.[2] It connects organic azide and terminal alkyne into 1,4-disubstituted 1,2,3-triazole, referred to as "click triazole".[3] Whereas click triazole has been frequently designed as an interconnector between two functional entities, its potential to offer a platform for further functionalization, e.g., via coordination to metals, still remains largely underexplored. In particular, there are only a handful of examples in which this triazole coordinates to a metal through the N2 nitrogen atom, being either a monodentate ligand or part of a polydentate chelator.

Considering the click triazole containing polydentate chelator, based on the position of the pendant coordinating group, coordination of the triazole can involve either the N3 or N2 nitrogen atom (Figure 1). These two isomeric click-triazole chelators will hereafter be referred to as chelators **A** and **B**, respectively. Having pendant primary amine groups, both isomeric click-triazole chelators have initially been examined as ligands for Re, ^{99m}Tc,[4] and Pt^{II}.[5] While chelators **A** formed stable complexes, this was not the case for isomers **B**.[4,5] Addressed by density functional theory (DFT) calculations, this difference has been accounted for by different electron densities at the triazole nitrogen atoms N3 and N2, with the latter being lower.[4−6] Recent studies in which the coordinative properties of different click triazoles were examined as mono- and polydentate ligands are consistent with

*To whom correspondences should be addressed. E-mail: fdeprof@vub.ac.be (F.D.P.), janez.kosmrlj@fkkt.uni-lj.si (J.K.).

(1) (a) L'abbé, G. *Bull. Soc. Chim. Belg.* **1984**, *93*, 579–592. (b) Tornøe, C. W.; Christensen, C.; Meldal, M. *J. Org. Chem.* **2002**, *67*, 3057–3064. (c) Rostovtsev, V. V.; Green, L. G.; Fokin, V. V.; Sharpless, K. B. *Angew. Chem., Int. Ed.* **2002**, *41*, 2596–2599.

(2) For selected comprehensive review articles, see: Meldal, M.; Tornøe, C. W. *Chem. Rev.* **2008**, *108*, 2952–3015 and the Supporting Information.

(3) Kolb, H. C.; Finn, M. G.; Sharpless, K. B. *Angew. Chem., Int. Ed.* **2001**, *40*, 2004–2021.

(4) Mindt, T. L.; Struthers, H.; Brans, L.; Anguelov, T.; Schweinsberg, C.; Maes, V.; Tourwé, D.; Schibli, R. *J. Am. Chem. Soc.* **2006**, *128*, 15096–15097.

(5) Maisonial, A.; Serafin, P.; Traïkia, M.; Debiton, E.; Théry, V.; Aitken, D. J.; Lemoine, P.; Viossat, B.; Gautier, A. *Eur. J. Inorg. Chem.* **2008**, 298–305.

(6) Bastero, A.; Font, D.; Pericàs, M. A. *J. Org. Chem.* **2007**, *72*, 2460–2468.

(7) For selected click triazole-based chemosensors, see: (a) Steinmetz, V.; Couty, F.; David, O. R. P. *Chem. Commun.* **2009**, 343–345. (b) Hung, H.-C.; Cheng, C.-W.; Ho, I.-T.; Chung, W.-S. *Tetrahedron Lett.* **2009**, *50*, 302–305. (c) Park, S. Y.; Yoon, J. H.; Hong, C. S.; Souane, R.; Kim, J. S.; Matthews, S. E.; Vicens, J. *J. Org. Chem.* **2008**, *73*, 8212–8218. (d) Varazo, K.; Xie, F.; Gulledge, D.; Wang, Q. *Tetrahedron Lett.* **2008**, *49*, 5293–5296. (e) Colasson, B.; Save, M.; Milko, P.; Roithová, J.; Schröder, D.; Reinaud, O. *Org. Lett.* **2007**, *9*, 4987–4990.

Published on Web 05/04/2010

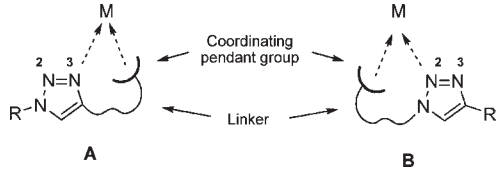

Figure 1. Schematic representation of the two isomeric click-triazole chelators **A** and **B**. Providing a short linker, chelation to metal M (depicted by dashed arrows) involves coordination of a pendant group and the triazole N3 and N2 atoms, respectively.

these observations.[7−10] Although, in some instances, N2 coordination has been suggested through different spectroscopic methods, only a few examples exist in copper coordination spheres in which the click-triazole N2 coordination is confirmed by X-ray.[11,12]

Herein we report that replacing the pendant primary amine group at the triazole N1 atom with an appropriate pyridine group dramatically improves the chelating properties of ligands **B**. This is exemplified by model compound $\mathbf{L}_x$ [1-(2-picolyl)-4-phenyl-1*H*-1,2,3-triazole; Chart 1] and its complexes with Pt^{II}, Pd^{II}, Cu^{II}, Ru^{II}, and Ag^{I}. These metal ions were selected to probe potentially different coordination numbers and geometries, as well as on the basis of their chemical and biochemical relevance. To shed light on the nature of coordinating properties of pyridine- and alkylamine-functionalized chelators **B** and to make a comparison with isomers **A**, compounds $\mathbf{L}_x$, $\mathbf{L}_y$ [1-(2-aminoethyl)-4-phenyl-1*H*-1,2,3-triazole], and $\mathbf{L}_z$ [4-(2-aminoethyl)-1-phenyl-1*H*-1,2,3-triazole; Chart 1] and their complexes with the above metal ions were investigated by density functional theory (DFT).

Experimental Section

General Procedures. NMR spectra were recorded at 302 K on a Bruker Avance DPX 300 spectrometer operating at 300, 282, 75, and 64 MHz for ^{1}H, ^{19}F, ^{13}C, and ^{195}Pt NMR, respectively. ^{1}H NMR spectra were referenced to tetramethylsilane (TMS) as the internal standard. Carbon chemical shifts were determined relative to the residual signal of dimethylformamide (DMF)-d_7 at δ 30.1 ppm. ^{195}Pt and ^{19}F NMR spectra were referenced to $Na_2[PtCl_6]$ and CCl_3F as external standards, respectively, at δ 0 ppm. Chemical shifts are given on the δ scale (ppm). Coupling constants (J) are given in hertz. Assignments of proton and carbon resonances were performed by standard 2D NMR techniques. The numbering used for the assignment of NMR signals is as follows: pyridine ring, simple figures; 1,2,3-triazole ring, primed figures; phenyl ring, double-primed figures; aromatic ring of *p*-cymene (in **4**), triple-primed figures. Mass spectra and high-resolution mass spectra were obtained with a VG-Analytical AutospecQ instrument and Q-TOF Premier instrument. Data are reported as m/z (relative intensity). IR spectra were recorded on a Bio-rad Excalibur Series spectrophotometer. Elemental analyses (C, H, and N) were performed with a Perkin-Elmer 2400 series II CHNS/O analyzer. Melting points were determined on a Kofler block.

Chart 1. Structures of Investigated Pyridine ($\mathbf{L}_x$)[a,b] and Primary Amine ($\mathbf{L}_y$)[a,b] Chelators **B** and Primary Amine ($\mathbf{L}_z$)[b] Chelator **A**, with a Selected Atom Numbering Scheme

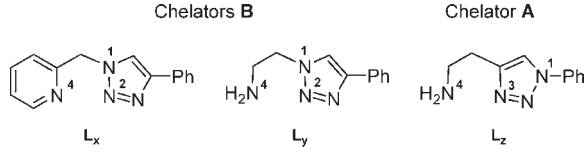

[a] Experimentally investigated. [b] Computationally investigated.

X-ray Structural Analysis. Crystal data and refinement parameters of compound **1**−**5** are listed in Table 1 and those for $\mathbf{L}_x$ in Table S1 of the Supporting Information. Single-crystal X-ray diffraction data of $\mathbf{L}_x$ and complexes **1**−**5** were collected with a Nonius Kappa CCD diffractometer with graphite-monochromated Mo Kα radiation (λ = 0.710 73). A Cryostream Cooler (Oxford Cryosystems) was used for cooling the samples of **2** and **3**. The data were processed by using *DENZO*.[13] The structures were solved by direct methods (*SIR-92*)[14] and refined by a full-matrix least-squares procedure based on F^2 (*SHELXL-97*).[15] All non-hydrogen atoms were refined anisotropically, while the hydrogen atoms were included in the model at geometrically calculated positions and refined by using a riding model. The water hydrogen atoms in **3** were not located. Compounds $\mathbf{L}_x$ and **3** crystallize in the noncentrosymmetric space groups. The value of the Flack parameter 0.473(13) of **3** indicates possible racemic twinning.

Computational Details. Geometry optimizations and frequency analysis were performed using the B3LYP method,[16] using the *Gaussian 03*[17] software package. For light atoms (H, N, and C), the aug-cc-pVDZ[18] basis set was used. For the transition metals M = Cu, Pd, and Ag, the aug-cc-pVDZ-pp[19] basis with a relativistic effective core potential was used; in the case of platinum, the double-ζ quality Def2-SVP basis[20] involving quasi-relativistic 60-electron core potential was used. All structures were verified to be minima on the potential energy

(8) For pyridine-conjugated click triazoles as chelators, see: (a) Nadler, A.; Hain, C.; Diederichsen, U. *Eur. J. Org. Chem.* **2009**, 4593–4599. (b) Schweinfurth, D.; Pattacini, R.; Strobel, S.; Sarkar, B. *Dalton Trans.* **2009**, 9291–9297. (c) Obata, M.; Kitamura, A.; Mori, A.; Kameyama, C.; Czaplewska, J. A.; Tanaka, R.; Kinoshita, I.; Kusumoto, T.; Hashimoto, H.; Harada, M.; Mikata, Y.; Funabiki, T.; Yano, S. *Dalton Trans.* **2008**, 3292–3300. (d) Schweinfurth, D.; Hardcastle, K. I.; Bunz, U. H. F. *Chem. Commun.* **2008**, 2203–2205. (e) Camp, C.; Dorbes, S.; Picard, C.; Benoist, E. *Tetrahedron Lett.* **2008**, *49*, 1979–1983. (f) Ziegler, T.; Hermann, C. *Tetrahedron Lett.* **2008**, *49*, 2166–2169. (g) Richardson, C.; Fitchett, C. M.; Keene, F. R.; Steel, P. J. *Dalton Trans.* **2008**, 2534–2537. (h) Meudtner, R. M.; Ostermeier, M.; Goddard, R.; Limberg, C.; Hecht, S. *Chem.—Eur. J.* **2007**, *13*, 9834–9840. (i) David, O.; Maisonneuve, S.; Xie, J. *Tetrahedron Lett.* **2007**, *48*, 6527–6530. (j) Huang, S.; Clark, R. J.; Zhu, L. *Org. Lett.* **2007**, *9*, 4999–5002. See also ref 12.

(9) For a survey of the Cambridge Structural Database, revealing very few reports of 1,2,3-triazole N2 coordination compounds, see the Supporting Information. See also: Moore, D. S.; Robinson, S. D. *Adv. Inorg. Chem.* **1988**, *32*, 171–239.

(10) For a recent comprehensive review article, see: Struthers, H.; Mindt, T. L.; Schibli, R. *Dalton. Trans.* **2010**, *39*, 675–696.

(11) The first X-ray evidence for click triazole N2 coordination to the metal has been provided for a dinuclear Cu^{I} complex with TBTA {$[Cu^{I}_2(\mu$-TBTA-κ^4-N^2,N^3,$N^{3\prime}$,$N^{3\prime\prime}$)$_2]^{2+}$; TBTA = tris(benzyltriazolylmethyl)amine}. See: Donnelly, P. S.; Zanatta, S. D.; Zammit, S. C.; White, J. M.; Williams, S. J. *Chem. Commun.* **2008**, 2459–2461.

(12) Brotherton, W. S.; Michaels, H. A.; Simmons, J. T.; Clark, R. J.; Dalal, N. S.; Zhu, L. *Org. Lett.* **2009**, *11*, 4954–4957.

(13) Otwinowski, Z.; Minor, W. *Methods Enzymol.* **1970**, *276*, 307–326.

(14) SIR92—A Program for Crystal Structure Solution: Altomare, A.; Cascarano, G.; Giacovazzo, C.; Guagliardi, A. *J. Appl. Crystallogr.* **1993**, *26*, 343–350.

(15) SHELXL-97—A program for Crystal Structure Refinement: Sheldrick, G. M. *Acta Crystallogr.* **2008**, *A64*, 112–122.

(16) (a) Becke, A. D. *J. Chem. Phys.* **1993**, *98*, 5648–5652. (b) Lee, C.; Yang, W.; Parr, R. G. *Phys. Rev. B* **1988**, *37*, 785–789.

(17) Frisch, M. J.; et al. *Gaussian 03*, revision B.03; Gaussian, Inc.: Pittsburgh, PA, 2003.

(18) Woon, D. E.; Dunning, T. H., Jr. *J. Chem. Phys.* **1993**, *98*, 1358–1371.

(19) (a) Peterson, K. A.; Puzzarini, C. *Theor. Chem. Acc.* **2005**, *114*, 283–296. (b) Figgen, D.; Rauhut, G.; Dolg, M.; Stoll, H. *Chem. Phys.* **2005**, *311*, 227–244.

(20) (a) Weigend, F.; Ahlrichs, R. *Phys. Chem. Chem. Phys.* **2005**, *7*, 3297–3305. (b) Andrae, D.; Haeussermann, U.; Dolg, M.; Stoll, H.; Preuss, H. *Theor. Chim. Acta* **1990**, *77*, 123–141.

Table 1. Experimental Data from the X-ray Diffraction Studies of Compounds **1**−**5**

	1	**2**	**3**	**4**	**5**
formula	$C_{14}H_{12}Cl_2N_4Pt$	$C_{32}H_{30}B_2F_8N_{10}Pd$	$C_{28}H_{28}Cl_2CuN_8O_2$	$C_{25}H_{26}ClF_3N_4O_3RuS$	$C_{28}H_{24}Ag_2N_{10}O_6$
fw (g mol^{-1})	502.27	834.68	643.02	656.08	812.31
cryst size (mm)	0.58 × 0.15 × 0.08	0.15 × 0.15 × 0.05	0.20 × 0.10 × 0.05	0.20 × 0.05 × 0.05	0.60 × 0.10 × 0.10
cryst color	colorless	yellow	green	yellow	colorless
cryst syst	monoclinic	triclinic	orthorhombic	monoclinic	monoclinic
space group	$P2_1/a$	$P\bar{1}$	$P2_1ca$	$P2_1/a$	$P2_1/c$
a (Å)	9.3229(2)	9.5792(3)	8.4365(1)	11.7266(3)	11.2169(2)
b (Å)	9.2897(3)	9.6228(2)	12.5126(2)	18.6948(5)	9.4764(2)
c (Å)	17.4537(5)	11.0935(3)	26.1418(3)	12.1187(2)	14.7408(3)
α (deg)	90	67.954(2)	90	90	90
β (deg)	92.992(2)	67.976(1)	90	93.603(2)	103.0982(9)
γ (deg)	90	73.081(2)	90	90	90
V (Å^3)	1509.55(7)	865.11(4)	2759.59(6)	2651.49(11)	1526.12(5)
Z	4	1	4	4	2
T (K)	293(2)	150(2)	150(2)	293(2)	293(2)
calcd density (g cm^{-3})	2.210	1.602	1.548	1.644	1.768
F(000)	944	420	1324	1328	808
no. of collected reflns	15147	10333	24792	39185	22089
no. of indep reflns	3268	3908	6095	6067	3472
R_{int}	0.039	0.023	0.052	0.052	0.033
no. of reflns used	2905	3827	5235	4373	2921
no. of param	190	242	370	346	208
R1 [$I > 2\sigma(I)$][a]	0.0285	0.0309	0.0427	0.0562	0.0321
wR_2 (all data)[b]	0.0800	0.1058	0.1041	0.1676	0.0811
GOF, S[c]	1.039	1.257	1.012	1.033	1.054
max/min residual electron density (e Å^{-3})	+1.64/−1.47	+0.92/−1.05	+0.34/−0.44	+1.23/−1.33	+0.41/−0.96

[a] $R1 = \sum||F_o| - |F_c||/\sum F_o|$. [b] $wR2 = \{\sum[w(F_o^2 - F_c^2)^2]/\sum[w(F_o^2)^2]\}^{1/2}$. [c] $S = \{\sum[(F_o^2 - F_c^2)^2]/(n/p)\}^{1/2}$ where n is the number of reflections and p is the total number of parameters refined.

surface, and the stability of the wave function was verified in all cases. For details on the calculations of complexation energies, inclusion of the effect of the solvent, and energy decomposition analysis, we refer to the Supporting Information.

Natural population analysis[21] was carried out on all complexes with the NBO program implemented in *Gaussian 03*. NBO charges, Wiberg bond indices,[22] and nucleus independent chemical shift (NICS)[23] values were determined at the B3LYP/aug-cc-pVDZ[24] level of theory. The latter were used to probe the aromaticity of the rings in the coordinating molecules and were evaluated in the center of the different unsaturated rings (1,2,3-triazole, pyridine, and phenyl ring) using the GIAO method.[25]

Synthesis. Reagents and solvents were used as purchased (Fluka, Aldrich, Alfa Aesar). 2-Picolylazide,[26] 1-azido-2-aminoethane,[27] 1-(2-aminoethyl)-4-phenyl-1*H*-1,2,3-triazole (**L**$_y$),[28] [$PtCl_2$COD][29] (COD = 1,5-cyclooctadiene), and *cis*-[$PtCl_2(DMSO)_2$][30] were prepared by literature procedures. Azides can be explosive, and caution should be exercised when handling them.[31]

1-(2-Picolyl)-4-phenyl-1*H*-1,2,3-triazole (L$_x$). A mixture of phenylacetylene (1.02 g, 10.0 mmol), 2-picolylazide (1.36 g, 10.1 mmol), $CuSO_4 \cdot 5H_2O$ (216 mg, 0.865 mmol), and granular copper (2.00 g, 31.5 mmol) in MeOH/water (20 mL/10 mL) was stirred for 1.5 h. The reaction mixture was filtered and diluted with saturated aqueous NH_4Cl (50 mL), and the product was extracted with CH_2Cl_2 (3 × 20 mL). The combined organic layers were washed with saturated aqueous NH_4Cl (3 × 20 mL) and brine (10 mL), dried over Na_2SO_4, and filtered. The solvent of the filtrate was removed in vacuo to give pure **L**$_x$ (2.19 g, 93%). Spectral and analytical data are given in the Supporting Information and are in agreement with those reported very recently.[12]

[$PtCl_2$L$_x$] (1). A mixture of **L**$_x$ (118 mg, 0.500 mmol) and *cis*-[$PtCl_2(DMSO)_2$] (224 mg, 0.500 mmol) in CH_2Cl_2 (8 mL) was stirred in the dark for 13 days. The product was collected by filtration and washed with CH_2Cl_2 (3 mL) to give pure **1** (198 mg, 0.395 mmol, 80%): pale-yellow solid, mp >300 °C. Anal. Calcd for $C_{14}H_{12}Cl_2N_4Pt$: C, 33.48; H, 2.41; N, 11.16. Found: C, 33.09; H, 2.48; N, 10.77. IR (KBr): ν 3105, 3086, 3031, 1612, 1477, 1432, 975, 768, 693 cm^{-1}. ^{1}H NMR (300 MHz, DMF-d_7): δ 6.32 (s, 2H, CH_2), 7.40−7.55 (m, 3H, H-3″, H-4″, H-5″), 7.73 (ddd, J = 1.7, 5.9, and 7.6 Hz, 1H, H-5), 7.88−7.94 (m, 2H, H-2″, H-6″), 7.99−8.03 (m, 1H, H-3), 8.29 (ddd, J = 1.4, 7.7, and 7.7 Hz, 1H, H-4), 9.21 (s, 1H, H-5′), 9.29 (dd, J = 1.4 and 5.9 Hz, 1H, H-6). ^{13}C NMR (75 MHz, DMF-d_7): δ 55.6 (CH_2), 126.27 (C-5′), 126.32 (C-2″, C-6″), 127.3 (C-5), 127.4 (C-3), 129.73 (C-1″), 129.77 (C-3″, C-5″), 129.9 (C-4″), 141.3 (C-4), 148.8 (C-4′), 151.6 (C-2), 154.4 (C-6). ^{195}Pt NMR (64 MHz, DMF-d_7): δ −2205. MS (ESI$^+$, %): m/z 525.0 ([Pt**L**$_x$$Cl_2$ + Na^+]$^+$, 100). Crystals suitable for X-ray analysis were prepared from a DMF-d_7 (0.5 mL) solution of **1** (20 mg). A few drops of diethyl ether were added into this solution until turbidity was observed. The resulting mixture was filtered, and the filtrate was aged at room temperature for few days to give pale-yellow crystals of **1**.

[Pd(L$_x$)$_2$](BF$_4$)$_2$·2CH$_3$CN (2·2CH$_3$CN). Ligand **L**$_x$ (189 mg, 0.800 mmol) was added to a solution of [$Pd(CH_3CN)_4$](BF_4)$_2$

(21) (a) Carpenter, J. E.; Weinhold, F. *J. Mol. Struct.* (*Theochem*) **1988**, *169*, 41–62. (b) Reed, A. E.; Curtiss, L. A.; Weinhold, F. *Chem. Rev.* **1988**, *88*, 899–926.
(22) Wiberg, K. *Tetrahedron* **1968**, *24*, 1083–1096.
(23) Schleyer, P. R.; Maerker, C.; Dransfeld, A.; Jiao, H. J.; Hommes, N. *J. Am. Chem. Soc.* **1996**, *118*, 6317–6318.
(24) For transition metals, aug-cc-pVDZ-cc (M = Cu, Ru, Pd, Ag) and Def2-SVP (M = Pt) were used.
(25) Ditchfield, R. *Mol. Phys.* **1974**, *27*, 789–807.
(26) Spencer, L. P.; Altwer, R.; Wei, P.; Gelmini, L.; Gauld, J.; Stephan, D. W. *Organometallics* **2003**, *22*, 3841–3854.
(27) Benalil, A.; Carboni, B.; Vaultier, M. *Tetrahedron* **1991**, *47*, 8177–8194.
(28) Urankar, D.; Steinbücher, M.; Kosjek, J.; Košmrlj, J. *Tetrahedron* **2010**, *66*, 2602–2613.
(29) Baker, M. V.; Brown, D. H.; Simpson, P. V.; Skelton, B. W.; White, A. H.; Williams, C. C. *J. Organomet. Chem.* **2006**, *691*, 5845–5855.
(30) Romeo, R.; Scolaro, L. M. *Inorg. Synth.* **1998**, *32*, 153–158.
(31) Bräse, S.; Gil, C.; Knepper, K.; Zimmermann, V. *Angew. Chem., Int. Ed.* **2005**, *44*, 5188–5240.

(178 mg, 0.400 mmol) in acetonitrile (10 mL) under stirring. A clear solution was obtained, from which after 10 min product started to crystallize. The reaction mixture was stirred overnight. The product was collected by filtration and washed with acetonitrile (1 mL) to give $\mathbf{2}\cdot 2CH_3CN$ (192 mg, 0.240 mmol, 60%). For this compound, it proved very difficult to remove traces of an unidentified compound, which was based on NMR spectra present as a ~10% impurity in the sample studied. The impurity was present even after several consecutive recrystallizations from different solvents, including water, acetonitrile, and ethanol as well as their mixtures: off-white solid, mp 263−266 °C. IR (KBr): ν 3142, 1612, 1476, 1443, 1081, 1034, 973, 766, 696 cm^{-1}. ^1H NMR (300 MHz, DMF-d_7): δ 6.99 (br s, 2H, CH_2), 7.46−7.59 (m, 3H, H-3″, H-4″, H-5″), 7.90−8.00 (m, 3H, H-5, H-2″, H6″), 8.24 (d, J = 7.8 Hz, 1H, H-3), 8.49 (ddd, J = 1.3, 7.7, and 7.7 Hz, 1H, H-4), 9.22 (br s, 1H, H-6), 9.49 (s, 1H, H-5′). ^{13}C NMR (75 MHz, DMF-d_7): δ 1.0 ($\underline{C}H_3CN$), 55.5 (CH_2), 118.2 ($CH_3\underline{C}N$), 126.5 (C-2″, C-6″), 127.6 (C-5), 128.2 (C-3), 128.5 (C-5′), 129.1 (C-1″), 130.0 (C-3″, C-5″), 130.5 (C-4″), 143.7 (C-4), 150.6 (C-4′), 152.2 (C-2), 155.2 (C-6). ^{19}F NMR (282 MHz, DMSO-d_6): δ 191.7. MS (ESI^+, %): m/z 615.1 ($[(Pd(\mathbf{L}_x)_2)^{2+} + Cl^-]^+$, 100). HRMS ($ESI^+$). Calcd for $C_{28}H_{24}{}^{35}ClN_8{}^{106}Pd^+$ ($[(Pd(\mathbf{L}_x)_2)^{2+} + Cl^-]^+$): 613.0847. Found: 613.0873. Crystals of $\mathbf{2}\cdot 2CH_3CN$ suitable for X-ray analysis were obtained by careful layering of acetonitrile solutions of $\mathbf{L}_x$ and $[Pd(CH_3CN)_4](BF_4)_2$ (2:1) and quiet aging of the resulting mixture for few days.

[$CuCl_2(\mathbf{L}_x)_2$] (3). A solution of $CuCl_2$ (36.0 mg, 0.268 mmol) in MeOH (1 mL) was added into a solution of ligand $\mathbf{L}_x$ (127 mg, 0.538 mmol) in MeOH (1 mL). The resulting mixture was stirred for 24 h, and the product was collected by filtration and washed with MeOH (1 mL) and diethyl ether (1 mL) to give pure **3** (129 mg, 0.213 mmol, 78%): blue crystals, mp 164−165 °C. Anal. Calcd for $C_{28}H_{24}Cl_2CuN_8$: C, 55.40; H, 3.99; N, 18.46. Found: C, 55.16; H, 3.88; N, 18.36. IR (KBr): ν 3120, 3034, 2998, 1608, 1573, 1485, 1469, 1432, 1227, 1078, 829, 760, 721, 694 cm^{-1}. MS (ESI^+, %): m/z 570.1 ($[M - Cl^-]^+$, 4), 535.1 (8), 259.1 (15), 237.1 (100). To prepare crystals suitable for X-ray analysis, product **3** (30 mg) was dissolved in hot EtOH (25 mL, 50 °C), followed by the addition of distilled water (10 mL). Upon isothermal evaporation of the solvents for a few weeks, crystals of $\mathbf{3}\cdot 2H_2O$ were grown.

[RuCl(η^6-*p*-cymene)$\mathbf{L}_x$]Cl (4′). A mixture of $\mathbf{L}_x$ (236 mg, 1.00 mmol) and [RuCl(μ-Cl)(η^6-*p*-cymene)]$_2$ (307 mg, 0.501 mmol) was stirred in absolute EtOH (50 mL) at room temperature for 2 days. Hexane was added under stirring until a slight turbidity was observed. The mixture was left to stand at 4 °C for 2 h and filtered, and then the volatiles of the filtrate were evaporated on a rotary evaporator to give **4′** (541 mg, 0.997 mmol, 100%) as an orange solid, mp 137−141 °C. IR (KBr): ν 3125, 3055, 2962, 1608, 1427, 1435, 1385, 1089, 769, 697 cm^{-1}. ^1H NMR (300 MHz, $CDCl_3$): δ 1.37 (d, J = 6.9 Hz, 3H), 1.41 (d, J = 6.9 Hz, 3H), 2.07 (s, 3H), 2.87−3.02 (m, 1H), 5.82 (d, J = 5.7 Hz, 1H), 6.11 (d, J = 5.7 Hz, 1H), 6.12 (d, J = 5.7 Hz, 1H), 6.39 (d, J = 5.7 Hz, 1H), 6.72 (d, J = 15.9 Hz, 1H), 7.08 (d, J = 15.9 Hz, 1H), 7.32−7.48 (m, 4H), 7.76−7.83 (m, 2H), 7.87 (ddd, J = 1.4, 7.6, and 7.6 Hz, 1H), 8.07 (d, J = 7.6 Hz, 1H), 9.01 (s, 1H), 9.03 (dd, J = 1.4 and 5.8 Hz, 1H). MS (ESI^+, %): m/z 507.1 ([RuCl(η^6-*p*-cymene)$\mathbf{L}_x$]$^+$, 100), 471.1 ([RuCl(η^6-*p*-cymene)$\mathbf{L}_x$]$^+$ − HCl]$^+$, 38). HRMS (ESI^+). Calcd for $C_{24}H_{26}{}^{35}ClN_4{}^{102}Ru^+$ ([RuCl(η^6-*p*-cymene)$\mathbf{L}_x$]$^+$): 507.0889. Found: 507.0900.

[RuCl(η^6-*p*-cymene)$\mathbf{L}_x$]OTf (4). The above-prepared **4′** (305 mg, 0.562 mmol) was dissolved in acetonitrile (3 mL), and a solution of AgOTf (145 mg, 0.564 mmol, 1 equiv) in acetonitrile (2 mL) was added slowly under stirring. The reaction mixture was stirred for 10 min and filtered through a pad of Celite. The Celite pad was rinsed with acetonitrile (10 mL), and the filtrate was evaporated to dryness to give **4** as an orange solid (360 mg, 0.549 mmol, 98%). The product was redissolved in boiling EtOH (7 mL), and the resulting solution was left to stand at room temperature overnight. Red crystals (210 mg), suitable for X-ray analysis, were collected by filtration: orange crystals, mp 211−213 °C. Anal. Calcd for $C_{25}H_{26}ClF_3N_4O_3RuS$: C, 45.77; H, 3.99; N, 8.54. Found: C, 45.64; H, 3.96; N, 8.51. IR (KBr): ν 3037, 2965, 1474, 1275, 1264, 1224, 1151, 1032, 770, 637 cm^{-1}. ^1H NMR (300 MHz, DMF-d_7): δ 1.42 (d, J = 3.0 Hz, 3H, $C\underline{H}_3CH$), 1.44 (d, J = 3.0 Hz, 3H, $C\underline{H}_3CH$), 2.08 (s, 3H, $CH_3\underline{Ar}$), 2.98−3.14 (m, 1H, $(CH_3)_2\underline{C}H$), 5.96 (d, J = 15.8 Hz, 1H, CH_2), 6.04 (d, J = 6.1 Hz, 1H, $\underline{Ar}$), 6.20 (d, J = 6.1 Hz, 1H, Ar), 6.25 (d, J = 6.1 Hz, 1H, Ar), 6.33 (d, J = 6.1 Hz, 1H, Ar), 6.48 (d, J = 15.8 Hz, 1H, CH_2), 7.42−7.49 (m, 1H, H-4″), 7.50−7.58 (m, 2H, H-3″, H-5″), 7.76 (dd, J = 6.5 and 6.5 Hz, 1H, H-5), 7.90−7.96 (m, 2H, H-2″, H-6″), 8.0 (d, J = 7.8 Hz, 1H, H-3), 8.25 (ddd, J = 1.4, 7.7, and 7.7 Hz, 1H, H-4), 9.15 (s, 1H, H-5′), 9.24 (d, J = 5.2 Hz, 1H, H-6). ^{13}C NMR (75 MHz, DMF-d_7): δ 18.0 ($\underline{C}H_3Ar$), 22.2 ($\underline{C}H_3CH$), 22.3 ($\underline{C}H_3CH$), 31.5 (CH), 55.2 (CH_2), 83.6 (C-2‴ or C-6‴), 84.4 (C-6‴ or C-2‴), 86.4 (C-3‴ or C-5‴), 90.1 (C-5‴ or C-3‴), 102.6 (C-1‴), 105.9 (C-4‴), 122.1 (q, J = 322 Hz, CF_3), 126.1 (C-2″, C-6″), 126.7 (C-5), 127.1 (C-3), 127.5 (C-5′), 129.80 (C-3″, C-4″, C-5″), 129.84 (C-1″), 141.2 (C-4), 150.1 (C-4′), 154.2 (C-2), 159.1 (C-6). ^{19}F NMR (282 MHz, DMF-d_7): δ −79.1.

[$Ag_2(\mathbf{L}_x)_2(NO_3)_2$] (5). A solution of $AgNO_3$ (47.0 mg, 0.277 mmol) in MeOH (2 mL) was dropwise added under stirring into the solution of ligand $\mathbf{L}_x$ (64.2 mg, 0.272 mmol) in MeOH (1 mL). The reaction mixture was stirred for 24 h, and the precipitated solid was collected by filtration and washed with MeOH (2 × 1 mL) and diethyl ether (2 × 2 mL) to give analytically pure complex **5** (92.4 mg, 0.114 mmol, 82%): white solid, mp 187−189 °C. Anal. Calcd for $C_{28}H_{24}Ag_2N_{10}O_6$: C, 41.40; H, 2.98; N, 17.24. Found: C, 41.20; H, 2.88; N, 17.11. IR (KBr): ν 3124, 3094, 1592, 1385, 1079, 768, 755, 689 cm^{-1}. ^1H NMR (300 MHz, DMF-d_7): δ 6.02 (s, 4H, 2 × CH_2), 7.38 (t, J = 7.4 Hz, 2H, 2 × H-4″), 7.48 (dd, J = 7.4 and 7.4 Hz, 4H, 2 × H-3″, 2 × H-5″), 7.55 (dd, J = 7.0 and 5.5 Hz, 2H, H-5), 7.67 (d, J = 7.8 Hz, 2H, H-3), 7.96 (d, J = 7.4 Hz, 4H, 2 × H-2″, 2 × H-6″), 7.99−8.07 (m, 2H, 2 × H-4), 8.74 (br d, J = 4.9 Hz, 2H, 2 × H-6), 8.86 (s, 2H, 2 × H-5′). ^{13}C NMR (75 MHz, DMF-d_7): δ 56.1 (CH_2), 123.2 (C-5′), 124.5 (C-3), 124.8 (C-5), 126.1 (C-2″, C-6″), 128.9 (C-4″), 129.6 (C-3″, C-5″), 131.3 (C-1″), 139.4 (C-4), 148.2 (C-4′), 151.6 (C-6), 155.3 (C-2). MS (ESI^+, %): m/z 579.1 ($[M - 2NO_3^- - Ag^+]^+$, 2), 237.1 (100). Crystals suitable for X-ray analysis were prepared by recrystallization of the above product (78 mg) from boiling benzonitrile (1 mL). Spectral and analytical data for the recrystallized product (45 mg, mp 185−188 °C) were identical with those described for the crude product **5**.

Results and Discussion

As noted in the Introduction, in sharp contrast to the primary amine group containing chelators **A**, the isomeric compounds **B** do not readily form stable chelates. It is, however, anticipated that replacement of the pendant primary amine group at the triazole N1 position with pyridine (e.g., 2-picolyl) should improve the chelating properties of compounds **B** and thus stabilize its complexes. Unlike the sp^3-hybridized aminoalkyl group, pyridine is a π acceptor and, when coordinated, it should withdraw the electron density from the metal, rendering it more electrophilic and thus more susceptible for coordination with the electron-deficient N2 nitrogen atom.[32] To demonstrate this, we selected a simple model ligand $\mathbf{L}_x$ (Chart 1), which offers a

(32) (a) Summa, N.; Schiessl, W.; Puchta, R.; van Eikema Hommes, N.; van Eldik, R. *Inorg. Chem.* **2006**, *45*, 2948–2959. (b) Weber, C. F.; van Eldik, R. *Eur. J. Inorg. Chem.* **2005**, 4755–4761. (c) Hofmann, A.; Jaganyi, D.; Munro, O. Q.; Liehr, G.; van Eldik, R. *Inorg. Chem.* **2003**, *42*, 1688–1700.

Scheme 1. Synthesis of Ligand $\mathbf{L}_x$ and Complexes **1**−**5**

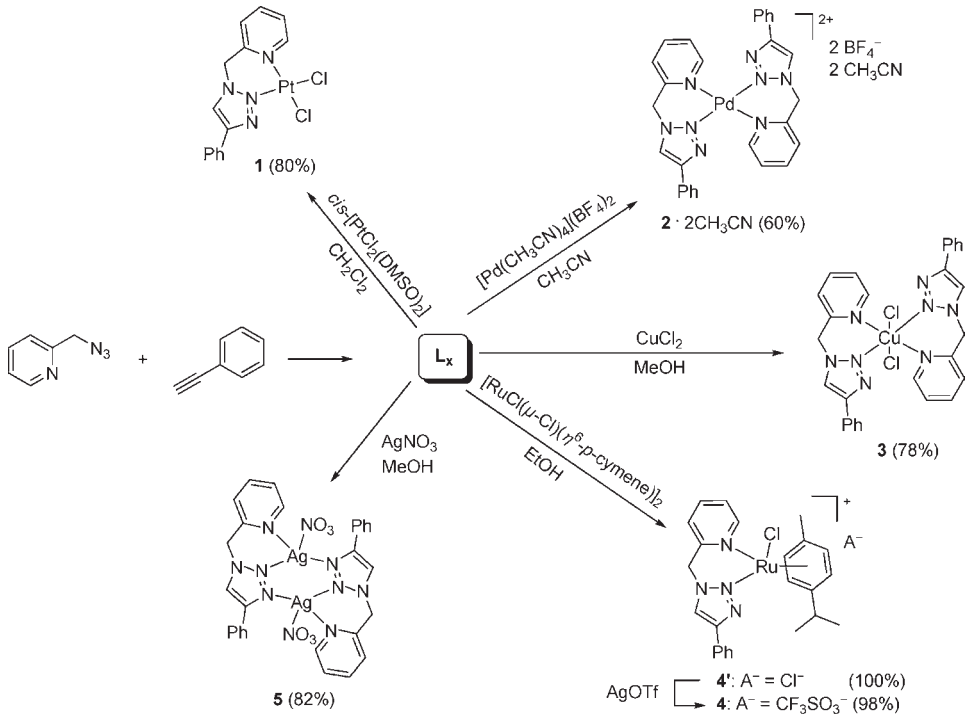

bidentate chelating system involving N2 of the 1,2,3-triazole and pyridine nitrogen atom. Ligand $\mathbf{L}_x$ was easily prepared by CuAAC reaction between phenylacetylene and 2-picolylazide as click components (Scheme 1).

The coordination of $\mathbf{L}_x$ to Pt^{II}, Pd^{II}, Cu^{II}, Ru^{II}, and Ag^{I} was examined with *cis*-$[PtCl_2(DMSO)_2]$, $[Pd(CH_3CN)_4](BF_4)_2$, $CuCl_2$, $[RuCl(\mu\text{-}Cl)(\eta^6\text{-}p\text{-cymene})]_2$, and $AgNO_3$ (Scheme 1). The syntheses of complexes **1**−**3** and **5** were surprisingly facile and were achieved by simple mixing of ligand $\mathbf{L}_x$ with a selected metal precursor in an equimolar ratio in an appropriate solvent at room temperature. In the case of $[Pd(CH_3CN)_4](BF_4)_2$ and $CuCl_2$, bisbidentate complexes **2** and **3** were obtained, respectively, and the syntheses of these two compounds were repeated with a $\mathbf{L}_x$/metal precursor molar ratio of 2:1. Pure stable products **1**−**3** and **5** crystallized out from the reaction mixtures and were isolated by filtration in 60−82% yield. More soluble Ru^{II} complex **4′** was prepared by the reaction between $\mathbf{L}_x$ and $[RuCl(\mu\text{-}Cl)(\eta^6\text{-}p\text{-cymene})]_2$ (2:1) and was isolated quantitatively by solvent evaporation.

The effect of the pendant group is clearly reflected in the coordination of platinum, which was previously shown not to form complexes with primary amine chelators **B**. For example, recent efforts to coordinate $\mathbf{L}_y$ either with K_2PtCl_4 or $KPtCl_3 \cdot DMSO$ as platinum sources were unsuccessful.[5,33] Our attempts to prepare platinum chelates from $\mathbf{L}_y$ and *cis*-$[PtCl_2(DMSO)_2]$ or $[PtCl_2COD]$ failed similarly.

We were also prompted to test whether the synthesis of the above complexes can be achieved in one pot from the corresponding phenylacetylene, 2-picolylazide, and the appropriate metal precursors without the ligand $\mathbf{L}_x$ isolation. This is potentially important for the synthesis and installation of metal chelates into biomolecules of diagnostic and therapeutic interest in a single step, if desired.[10] If successful, it would further demonstrate the chelating ability of ligand $\mathbf{L}_x$. Three-step, click−chelate−filtrate, one-pot, or telescoped reactions were conducted by using the above-mentioned reaction partners, affording pure complexes **1** (73%), **2** (90%), **3** (78%), and **5** (90%) in excellent yields (Supporting Information).

Crystals of products **1**−**3** and **5** suitable for X-ray analysis were prepared by recrystallization from the appropriate solvents, as described in the Experimental Section. Ruthenium complex **4′** was isolated as a glassy material, and crystals of $[RuCl(\eta^6\text{-}p\text{-cymene})\mathbf{L}_x]^+$ suitable for X-ray diffraction were prepared from its triflate salt **4**. It should be noted that while this paper was in preparation, Zhu et al.[12] reported the synthesis and crystal structure of $[Cu(\mathbf{L}_x)_2(CH_3CN)(ClO_4)](ClO_4)$ in which two ligands $\mathbf{L}_x$ are in bisbidentate fashion coordinated to Cu^{II}, analogously to **3**.

Complexes **1**−**5** were fully characterized by CHN analysis, ESI-MS, and 1D and 2D NMR spectroscopy. The NMR characterization of all of the complexes in solution was for the comparison reasons carried out in DMF-d_7. Other less polar organic solvents and water proved to be inappropriate because of solubility reasons, whereas dimethyl sulfoxide (DMSO-d_6) caused rapid ligand-exchange reactions at **1**. Bidentate coordination through the triazole N2 and pyridine N4 nitrogen atoms in **1**−**5** was confirmed by ^1H and ^{13}C NMR spectroscopy. In comparison to $\mathbf{L}_x$, significant downfield shifts in several ^1H NMR resonances were observed, especially for the H6 proton of the pyridine, the methylene group, and the H5 of the triazole (Figure 2). These observations are fully consistent with both heterocycles, triazole and pyridine, being involved in coordination to the metals. ^{195}Pt NMR spectrum of **1** showed a single resonance at δ −2205 ppm, confirming the N_2Cl_2 coordination set.[34] Methylenic

(33) It is of note that structurally similar chelator **A**, 4-(aminomethyl)-1-benzyl-1*H*-1,2,3-triazole, readily formed a stable five-membered Pt^{II} complex, which allowed characterization through X-ray diffraction; see ref 5.

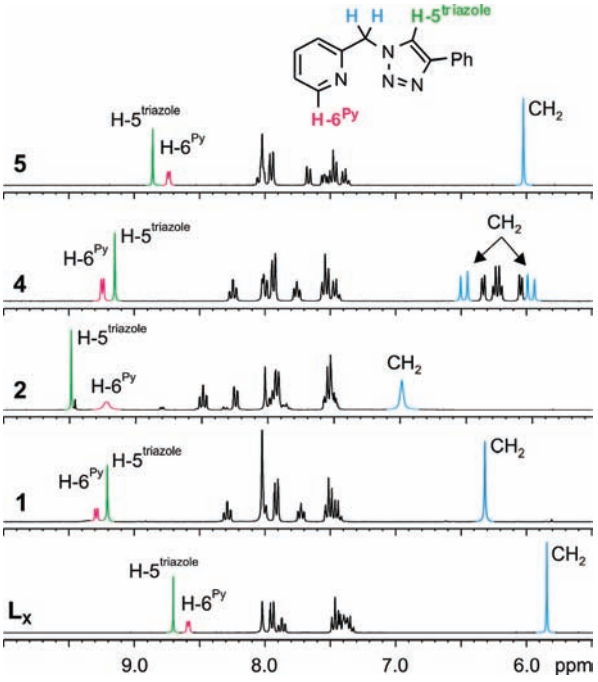

Figure 2. Low-field regions of the ^{1}H NMR spectra of $\mathbf{L}_x$, **1**, **2**, **4**, and **5** in DMF-d_7.

Table 2. Selected Bond Lengths (Å) and Angles (deg) for **1**−**5** from Crystallographic Data

		1	
Pt1−N2	1.997(4)	N2−Pt1−N4	88.75(16)
Pt1−N4	2.029(4)	N2−Pt1−Cl1	177.55(12)
Pt1−Cl1	2.2824(11)	N2−Pt1−Cl2	90.54(12)
Pt1−Cl2	2.2853(13)	N4−Pt1−Cl1	91.23(11)
		N4−Pt1−Cl2	178.82(11)
		Cl1−Pt1−Cl2	89.51(5)
		2	
Pd1−N2	2.0022(19)	N2−Pd1−N4	88.16(8)
Pd1−N4	2.035(2)		
		3	
Cu1−N2	2.385(3)	N2−Cu1−N4	86.90(10)
Cu1−N4	2.054(3)	N2′−Cu1−N4′	85.47(10)
Cu1−N2′	2.777(3)	N2−Cu1−Cl1	89.18(9)
Cu1−N4′	2.043(3)	N2−Cu1−Cl2	95.11(9)
Cu1−Cl1	2.3072(10)	N2−Cu1−N2′	177.53(11)
Cu1−Cl2	2.3278(11)	Cl1−Cu1−Cl2	175.68(4)
		4	
Ru1−N2	2.082(4)	N2−Ru1−N4	83.45(15)
Ru1−N4	2.115(4)	N2−Ru1−Cl1	85.38(11)
Ru1−Cl1	2.3785(12)	N4−Ru1−Cl1	83.97(12)
		5	
Ag1−N2	2.445(2)	N2−Ag1−N4	85.16(7)
Ag1−N4	2.277(2)	N2−Ag1−N3[a]	108.14(7)
Ag1−N3[a]	2.229(2)	N2−Ag1−O1	113.58(11)
Ag1−O1	2.447(3)		

[a] Symmetry code: i, $2 - x, -y, 1 - z$.

hydrogen atoms in **1**, **2**, and **5** appeared as singlets, which could be interpreted as a result of the dynamic behavior of the six-membered metallacycle, making equivalent both hydrogen atoms on the NMR time scale. The ^{1}H NMR spectrum of **4** displays a well-resolved AB spin system (δ 5.96 and 6.48 ppm, 2 × d, J = 15.8 Hz), and the apparent reason for such dynamic behavior is the sterical hindrance of ligand $\mathbf{L}_x$ exerted by cymene and chloride ligands. The paramagnetic complex **3** was not amenable to structural investigation by NMR spectroscopy.

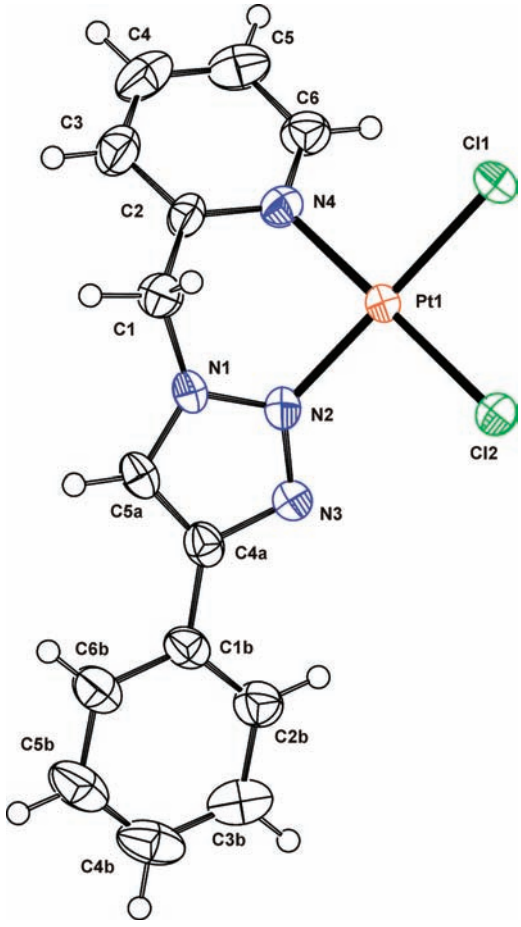

Figure 3. ORTEP view of **1** (thermal ellipsoids are at 50% probability).

Structural Studies. To confirm the chelation of $\mathbf{L}_x$, single-crystal X-ray analysis was undertaken. Selected bond lengths and angles for compounds **1**−**5** are summarized in Table 2. The molecular structures are shown in Figures 3−7. For the crystal structure of $\mathbf{L}_x$ and illustrations of $\pi-\pi$ stacking interactions in $\mathbf{L}_x$ and **1**−**4**, see Table S1 and Figures S1−S6 in the Supporting Information.

The structures of **1** and **2** exhibit a square-planar coordination environment of the central metal atom. The two nitrogen atoms of the ligand $\mathbf{L}_x$ and two chloride ions in the cis position fulfill the coordination sphere around the platinum atom in **1**, whereas the structure of **2** consists of a mononuclear bisbidentate complex where the palladium ion is trans-chelated by the two $\mathbf{L}_x$ molecules. The bond distances in the coordination sphere of platinum in **1** are comparable to those found in other square-planar complexes of Pt^{II}.[5] The diagonal bonds in **2** are nonequivalent, with N2−Pd1 being shorter than N4−Pd1.

(34) Still, B. M.; Kumar, P. G. A.; Aldrich-Wright, J. R.; Price, W. S. *Chem. Soc. Rev.* **2007**, *36*, 665–686.

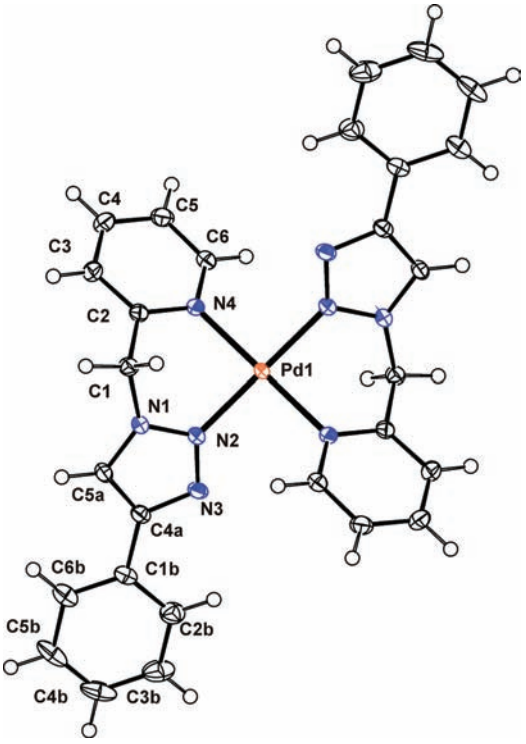

Figure 4. ORTEP view of $2 \cdot 2CH_3CN$ (thermal ellipsoids are at 50% probability). The BF_4^- ions and the lattice CH_3CN molecules have been removed for clarity.

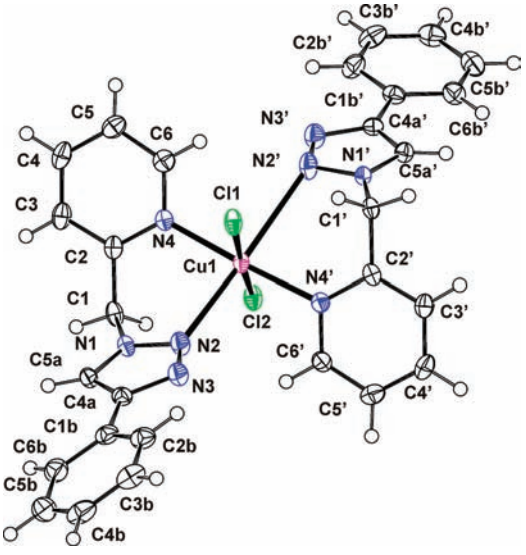

Figure 5. ORTEP view of $3 \cdot 2H_2O$ (thermal ellipsoids are at 50% probability). The lattice water molecules have been removed for clarity.

Similarly to **2**, in complex **3** the ligands $\mathbf{L}_x$ adopt a trans configuration. Regarding the bonding situation of $\mathbf{L}_x$, the structure of **3** is comparable to that of **2** except that in this case the metal ion is in a distorted octahedral coordination environment with two additional chloride ions involved. Severe distortion of this octahedron is found in the coordination geometry of axial N2 and N2′ atoms with Cu−N separations of 2.385(3) and 2.777(3) Å, respectively. This displacement of two axial N2 atoms from the basal plane formed by two pyridine N4 atoms and two chloride ions suggests a pyramidal distortion of

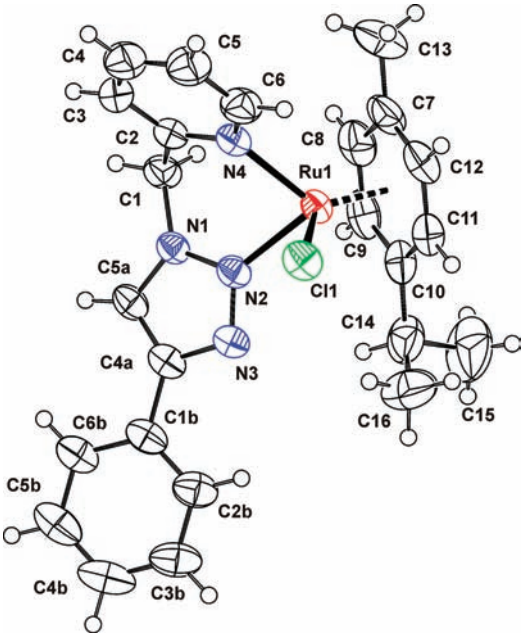

Figure 6. ORTEP view of **4** (thermal ellipsoids are at 50% probability). The $CF_3SO_3^-$ ion has been removed for clarity.

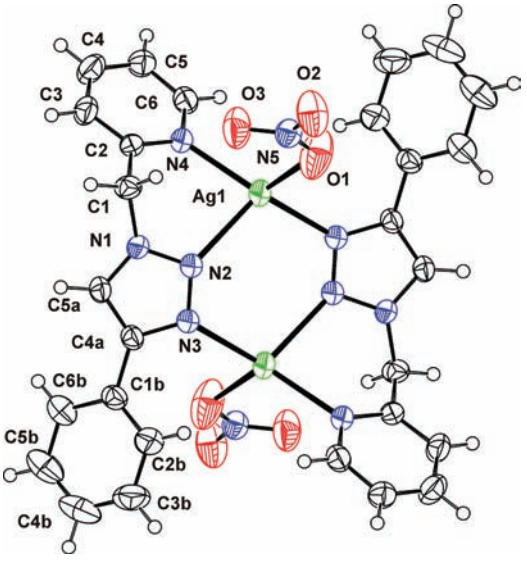

Figure 7. ORTEP view of **5** (thermal ellipsoids are at 50% probability).

the octahedral geometry. The distances between the copper atom and pyridine N4 atoms or chlorine atoms are in the normal ranges. The bonding geometry of $\mathbf{L}_x$ around the central copper atom is different from the recently reported ionic complex of $[Cu(\mathbf{L}_x)_2(CH_3CN)(ClO_4)](ClO_4)$,[12] where Cu^{II} displays the square-planar geometry of four nitrogen atoms with distant CH_3CN and ClO_4^- ligands at the axial positions.

The structure of **4** consists of a $[RuCl(\eta^6\text{-}p\text{-cymene})\mathbf{L}_x]^+$ cation and a $CF_3SO_3^-$ anion. The complex exhibits a three-legged piano-stool geometry with the metal center coordinated by *p*-cymene in a η^6 fashion, a chloride ion, and ligand $\mathbf{L}_x$. The distances between Ru^{II} and the nitrogen atoms of $\mathbf{L}_x$ are not equivalent, analogously to complexes **1** and **2**.

Complex **5** contains two silver centers that are bridged by two $\mathbf{L}_x$ molecules. Both metal ions in the structure are

Chart 2. Computationally Investigated $[\mathbf{ML}_n(\mathbf{NH_3})_2]^{2+}$ (M = Cu, Pd, Pt) and $[\mathbf{AgL}_n\mathbf{NH_3}]^+$ (n = x, y, z) Molecules with the Selected Atom Numbering Scheme

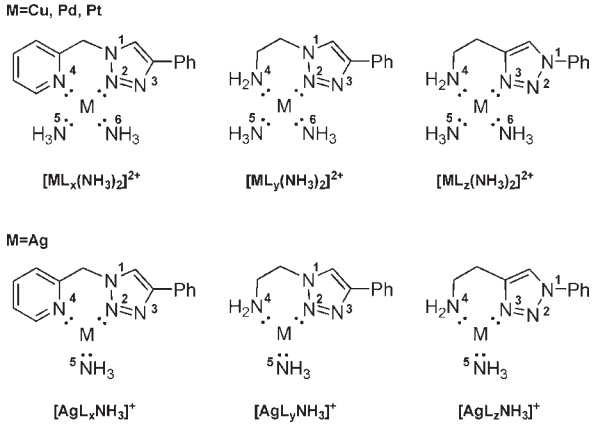

ligated by two nitrogen atoms from one $\mathbf{L}_x$ ligand (N4 from the pyridine and N2 from the triazole part) and another triazole N3 atom from the second $\mathbf{L}_x$ ligand in the complex. The distorted tetrahedral coordination is fulfilled by the oxygen atom of a nitrate anion coordinated to both silver atoms in a monodentate mode. Alternatively, coordination of the silver atoms can also be described as distorted trigonal planar, where each silver atom is displaced from the plane of the coordinating nitrogen atoms for 0.564 Å.

Within the aromatic system, relevant distortion was found when ligand $\mathbf{L}_x$ is bound to the metal center. Whereas in $\mathbf{L}_x$ the angle between the plane of the pyridine ring and the plane of the triazole ring is 87.7°, in complexes **1**−**5**, these angles are in the range from 131.4° in **1** to 114.4° in **3**. The planes of the triazole ring and that of the phenyl ring in $\mathbf{L}_x$ are almost coplanar. The angle between these rings is 11.37°, whereas in complexes **1**−**5**, these values expand from 5.98° in **1** to 31.76° in **5**. Accordingly, the bite angle N−M−N decreases from **1** (88.8°) to **4** (83.5°).

Theoretical Calculations. Ligands $\mathbf{L}_x$, $\mathbf{L}_y$, and $\mathbf{L}_z$ and the corresponding theoretically investigated complexes are depicted in Charts 1 and 2, respectively. In line with our experimental observations, the complexes with central atoms of copper, palladium, and platinum, $[\mathbf{ML}_n(\mathbf{NH_3})_2]^{2+}$ (M = Cu, Pd, Pt; n = x, y, z), were calculated with coordination number 4, while silver derivatives $[\mathbf{AgL}_n\mathbf{NH_3}]^+$ were modeled with coordination number 3. To put all of the results obtained on equal footing, only one-metal, one-ligand $\mathbf{L}_n$ (n = x, y, z) complexes were considered in which ammonia was used for ligands other than $\mathbf{L}_n$. Because the calculations returned the expected square-planar (M = Pd, Pt) and trigonal-planar (M = Ag) geometries with a singlet ground state, the applied substitution seems to be appropriate for addressing this issue (compare Tables 2 and 3).[35]

Stability of $\mathbf{L}_x$ Coordinated Complexes. Favorable gas-phase complexation energies (ΔE^{gas}) and Gibbs free energies (ΔG^{gas}) for coordination of the metal ion with ligand $\mathbf{L}_x$ and ammonia were computed with a stabilization of about 400−430 kcal mol^{-1} in most of the cases (Table S2 in the Supporting Information). The only exception was the silver derivative, for which the smallest stabilization, about 100 kcal mol^{-1}, was observed. As for the synthesis of compounds **1**−**5**, different polar and apolar solvents were employed including dichloromethane (DCM) and methanol, and complexation energies ΔG^{DCM} and ΔG^{MeOH} were calculated in the liquid phase (Table S2 in the Supporting Information). As expected, the complexation energies calculated in the liquid phase, especially in polar methanol, are greatly reduced with respect to the gas phase ΔG^{gas} values; however, the formation of all of the complexes is still favorable.[36]

Table 3. Selected Bond Lengths (Å) and Angles (deg) for $[\mathbf{ML}_x(\mathbf{NH_3})_2]^{2+}$ (M = Cu, Pd, Pt) and $[\mathbf{AgL}_x\mathbf{NH_3}]^+$ from Computational Data[a]

complex	M−N2	M−N4	N2−M−N4
$[\mathbf{PdL}_x(\mathbf{NH_3})_2]^{2+}$	2.00	2.07	88.3
$[\mathbf{CuL}_x(\mathbf{NH_3})_2]^{2+}$	1.98[36]	2.04	90.3
$[\mathbf{AgL}_x\mathbf{NH_3}]^+$	2.41	2.26	86.5
$[\mathbf{PtL}_x(\mathbf{NH_3})_2]^{2+}$	2.01	2.08	88.2

[a] For atom numbering, see Chart 2.

The natural bond orbital (NBO) analysis reveals that the main interactions in $[\mathbf{ML}_n(\mathbf{NH_3})_2]^{2+}$ (M = Cu, Pd, Pt) complexes are the donation of the in-plane lone pairs of the appropriate nitrogen atoms of ligand $\mathbf{L}_n$ and two ammonia (Chart 2) to the empty s and d orbitals of the metal, reducing the charge localized on the metal (Table 4). In contrast, because in the case of $[\mathbf{AgL}_n\mathbf{NH_3}]^+$ the d orbitals are filled, donation occurs only to the 5s orbital, resulting in a much weaker interaction between the ligands and the silver ion. This is in line with the above results that for these compounds the smallest stabilization energy was observed (Table S2 in the Supporting Information).

Chelators A and B Having Pendant Primary Amine Groups. As already mentioned in the literature, the charge on the triazole N3 nitrogen is significantly more negative from that of N2.[4−6,10] Accordingly, the higher stability of the complexes with chelators **A** (Figure 1) was attributed to this structural deviation. In contrast, in the series of the pendant primary amine analogues, our following analysis shows that the more efficient π-back-donation rather than electrostatic interactions makes complexes with ligand **A** more stable than those with isomer **B**.

From the NICS values for the triazole heterocycle and the phenyl ring, one can conclude that the back-donation to the triazole ring is notably more effective for $\mathbf{L}_z$ than for $\mathbf{L}_y$ (Table 4). For instance, in the case of platinum derivatives, the NICS value of the triazole (phenyl ring) is decreased by 1.63 (1.00) and 0.36 (0.58) for $\mathbf{L}_z$ and $\mathbf{L}_y$, respectively (compare entry 15 with entry 12 and entry 14 with entry 8) upon coordination, indicating a higher aromaticity of these rings in the complexes with $\mathbf{L}_z$ as compared to the rings in the complexes with $\mathbf{L}_y$. For the data and evaluation of the energy decomposition analysis that support this conclusion, see the Supporting Information.

Different bonding situations in the complexes with these two isomeric ligands can also be demonstrated within the MO ansatz. For example, unique bonding combinations formed by the d_{z^2} orbital of the metal (d_{z^2}

(35) Calculations were also performed on coordinationally unsaturated one-metal-one-ligand $[\mathbf{ML}_x]^{2+}$ (M = Cu, Ru, Pd, Pt) and $[\mathbf{ML}_x]^+$ (M = Ag) type complexes, but because the obtained geometries showed higher deviations from the experimental structures than those for the $[\mathbf{ML}_n(\mathbf{NH_3})_2]^{2+}$ and $[\mathbf{AgL}_n\mathbf{NH_3}]^+$ complexes, the former were not investigated further.

Table 4. NBO Charges and NICS Values for the Investigated Complexes and Ligands $\mathbf{L}_n$ (n = x, y, z)

		NBO charge				NICS[a]		
entry	structure	N2	N3	N4	M	triazole	pyridine	phenyl
				Complexes with Ligand $\mathbf{L}_x$				
1	$[CuL_x(NH_3)_2]^{2+}$	−0.26		−0.62	1.31	−9.05	−7.14	−5.38
2	$[AgL_xNH_3]^{+}$	−0.18		−0.59	0.76	−9.84	−6.29	−6.56
3	$[PdL_x(NH_3)_2]^{2+}$	−0.13		−0.51	0.83	−9.71	−6.90	−6.58
4	$[PtL_x(NH_3)_2]^{2+}$	−0.12		−0.50	0.76	−9.89	−7.05	−6.76
				Complexes with Ligand $\mathbf{L}_y$				
5	$[CuL_y(NH_3)_2]^{2+}$	−0.27		−0.96	1.30	−9.05		−5.70
6	$[AgL_yNH_3]^{+}$	−0.19		−0.95	0.75	−10.09		−6.49
7	$[PdL_y(NH_3)_2]^{2+}$	−0.14		−0.84	0.82	−9.80		−6.66
8	$[PtL_y(NH_3)_2]^{2+}$	−0.13		−0.83	0.75	−9.95		−6.70
				Complexes with Ligand $\mathbf{L}_z$				
9	$[CuL_z(NH_3)_2]^{2+}$		−0.45	−0.95	1.30	−10.75		−8.19
10	$[AgL_zNH_3]^{+}$		−0.41	−0.96	0.76	−10.82		−7.83
11	$[PdL_z(NH_3)_2]^{2+}$		−0.32	−0.84	0.82	−10.80		−8.34
12	$[PtL_z(NH_3)_2]^{2+}$		−0.31	−0.83	0.74	−10.91		−8.33
				Ligands				
13	$\mathbf{L}_x$	−0.07		−0.48		−9.62	−6.02	−6.58
14	$\mathbf{L}_y$	−0.08		−0.92		−9.59		−6.12
15	$\mathbf{L}_z$		−0.27	−0.92		−9.28		−7.33

[a] For comparison, the NICS value of benzene is −9.48.

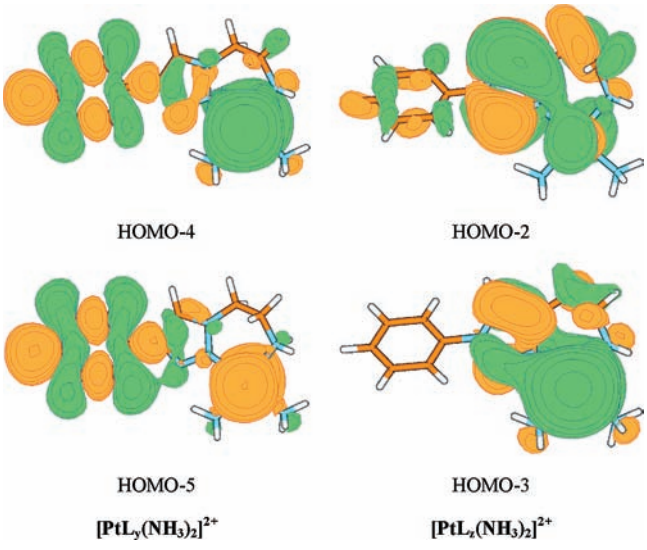

Figure 8. Representative orbitals showing the main difference between the isomeric primary amine containing chelates involving triazole N3 ($[PtL_z(NH_3)_2]^{2+}$) and N2 ($[PtL_y(NH_3)_2]^{2+}$) atoms (isovalue = 0.01 au).

is σ interacting in D_{4h} symmetry) and high-lying orbitals of the triazole ring can only be observed in $\mathbf{L}_z$ complexes

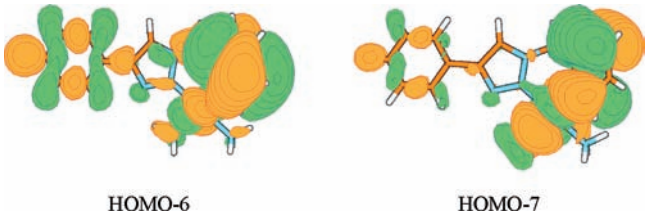

Figure 9. MOs representing the π-back-donation from the metal center to the pyridine side chain of the ligand in $[PtL_x(NH_3)_2]^{2+}$ (isovalue = 0.01 au).

(compare HOMO−2 and HOMO−3 of $\mathbf{L}_z$ and HOMO−4 and HOMO−5 of $\mathbf{L}_y$ in Figure 8).[37] These interactions result in more efficient delocalization of the metal d electrons to the π system of the ligand, increasing the aromaticity and thus the stability of the complexes with $\mathbf{L}_z$ (chelators **A**).

Comparison of Chelators B with Both a Pendant Primary Amine Group ($\mathbf{L}_y$) and a Pyridine Group ($\mathbf{L}_x$). Smaller differences in the NICS values at the triazole ring for $\mathbf{L}_x$ in comparison to $\mathbf{L}_y$ suggest a less efficient back-donation to this heterocycle at the former ligand (Table 4). However, the main difference between the stability of the complexes with these two ligands is the interaction of the metal with the π system of the pendant pyridine group (in $\mathbf{L}_x$). The NICS values calculated in the center of pyridine are decreased by an average of 0.82, which means significantly increased aromaticity during the coordination of $\mathbf{L}_x$ to the metal (for the Pt^{II} complex, compare entry 13 with entry 4). Second-order perturbation theory analysis of the Kohn−Sham matrix confirms this stabilization effect. MO theory provides again insight into the bonding situation between the metal center and the ligand, and it clearly shows delocalization of d

(36) For the copper analogue, which was calculated in its doublet ground state, we obtained the expected planar arrangement of the central N2−N4−Cu−N5−N6 segment, however, with a significantly shorter Cu−N2 bond distance (1.98 Å) than that observed by X-ray spectroscopy for **3** (2.385 and 2.777 Å). It is worth mentioning that the calculated value is in good agreement with that recently reported for $[Cu(\mathbf{L}_x)_2(CH_3CN)(ClO_4)](ClO_4)$ (2.003 and 2.007 Å) in ref 12.

(37) For ligand-exchange reactions, ΔG_R of tetraamine metal (M = Cu, Pd, Pt) and triamine metal (M = Ag) complexes, which yield the various chelates, $M(NH_3)_{z+2}^{z+} + L_n = ML_n(NH_3)_z^{z+} + 2NH_3$ (n = x, y, z). See the Supporting Information.

electrons into the π system of the pyridine moiety (Figure 9, HOMO−6 and HOMO−7). This causes higher aromaticity and stabilization of $\mathbf{L}_x$ complexes with respect to the $\mathbf{L}_y$ analogues and is consistent with the experimental results. It is also in agreement with the pyridine ring acting as a π-electron-withdrawing group.[32]

Conclusions

We demonstrated that, assisted by a pendant pyridine group, 1,2,3-triazole can form stable coordination with the N2 nitrogen atom. The structures of the chelates with Pt^{II}, Pd^{II}, Cu^{II}, Ru^{II}, and Ag^{I} were confirmed by X-ray diffraction, the first time for some metals. The bonding patterns and the electronic structures of the complexes were analyzed by DFT calculations using different techniques. In contrast to the previous suggestions that stronger electrostatic interaction results in stronger coordination, our calculations indicate that the stability difference is caused by the distinct magnitude of π-back-donation. The extra stabilization, which makes the complexes of $\mathbf{L}_x$ synthesizable, is evolved by delocalization of metal d electrons into the π system of the pyridine moiety of the ligand. It seems unlikely that this coordination is restricted to the pyridine heterocycle and the metal ions selected herein, and we believe that this work will stimulate future endeavors in the growing field of click chelates, especially in connection with their potential catalytic and biological activity, as well as chemosensors.[39]

(38) For the complete set of relevant orbitals, see Table S8 in the Supporting Information.

(39) For some preliminary endeavors in this direction from our laboratories, see: Urankar, D.; Košmrlj, J. *J. Comb. Chem.* **2008**, *10*, 981–985 and ref 28.

Acknowledgment. The authors are thankful for financial support from the Ministry of Higher Education, Science and Technology of the Republic of Slovenia and the Slovenian Research Agency (Grants P1-0230-0103 and P1-0175) and from a Research Program of the Research Foundation - Flanders (Grant G.0464.06). We thank Dr. Bogdan Kralj and Dr. Dušan Žigon (Mass Spectrometry Center, Jožef Stefan Institute, Ljubljana, Slovenia) for mass spectral measurements.

Supporting Information Available: Additional literature survey and experimental data, characterization and X-ray data for ligand $\mathbf{L}_x$, schematic representations of $\mathbf{L}_x$ and **1**−**5** showing $\pi-\pi$ stacking, computational details, NMR spectra, UV−vis spectra, and X-ray data for compounds $\mathbf{L}_x$ and **1**−**5** in CIF format. This material is available free of charge via the Internet at http://pubs.acs.org.